ELSEVIER

Journal of Physics and Chemistry of Solids 65 (2004) 1479–1484

JOURNAL OF PHYSICS AND CHEMISTRY OF SOLIDS

www.elsevier.com/locate/jpcs

Sc doping of MgB_2: the structural and electronic properties of $Mg_{1-x}Sc_xB_2$

S. Agrestini[a,*], C. Metallo[a], M. Filippi[a], G. Campi[a], C. Sanipoli[a], S. De Negri[b], M. Giovannini[b], A. Saccone[b], A. Latini[c], A. Bianconi[a]

[a]*Dipartimento di Fisica and Unità INFM, Università di Roma 'La Sapienza', P. le Aldo Moro 2, 00185 Roma, Italy*
[b]*Dipartimento di Chimica e Chimica Industriale, Università di Genova, Via Dodecaneso 31, 16146 Genova, Italy*
[c]*Dipartimento di Chimica, Università di Roma 'La Sapienza', P. le Aldo Moro 2, 00185 Roma, Italy*

Received 27 June 2003; revised 12 August 2003; accepted 5 September 2003

Abstract

We have investigated the effect of electron doping on the superconducting properties of MgB_2. For the purpose we have synthesized several samples along the $Mg_{1-x}Sc_xB_2$ section. The X-ray diffraction measurements reveal small changes in the lattice parameters suggesting that the Sc doping could be considered to simply fill the boron σ bands. Radio frequency surface resistivity measurements has been used to obtain the variation of T_c with Sc doping. Increasing the Sc content, the experimental T_c diverges from the T_c predicted by the BCS single band theory showing the key role of interchannel pairing near a shape resonance.

Keywords: A. Superconductivity

About 2 years ago, a great excitement in the solid state physics community was raised by the surprising discovery of superconductivity in the binary boride, MgB_2, with a T_c of about 39 K, which is the highest known transition temperature for a non-copper-oxide bulk material [1]. This discovery stimulated intense experimental and theoretical investigations [2] because of the apparent simplicity of MgB_2 with respect to its chemical composition, the crystal structure and the electronic properties and, in addition, due to missing complication related to strong electron–electron correlations. For this simplicity the understanding of superconductivity in this binary compound should be much easier than in the high T_c cuprate materials studied extensively for more than 15 years now.

On the other hand, the underlying mechanism of superconductivity in this compound is still an issue of current debate. In fact its critical temperature of about 39 K is close to or above the theoretical value predicted by the BCS theory [3]. This may be a strong argument to consider MgB_2 as a non-conventional superconductor.

Therefore, the question of fundamental importance is to determine the parameters that allow to explain the presence of the high T_c superconducting phase in MgB_2 with respect to other diborides having same lattice structure C32 that are not superconducting (like AlB_2) or have a low critical temperature.

The superconductivity in MgB_2 has been attributed to the conduction bands formed by boron layers [4–7], the electronic structure of which depends on several parameters:

1. the charge density in the boron layers;
2. the micro-strain of the B–B distance;
3. the spacing between the boron monolayers determined by the *c*-axis; and
4. the frequency ω_0 of the E_{2g} phonons

In particular the first parameter, i.e. the charge density in the boron layers, determines the position of the Fermi level related to the boron σ bands [5,8,9].

The second key parameter, the elastic micro-strain in the boron planes, is due to the lattice mismatch existing between the different layers [10,11]. This structural parameter

* Corresponding author. Fax: +39-6-495-7697.
E-mail address: stefano.agrestini@roma1.infn.it (S. Agrestini).

0022-3697/$ - see front matter © 2004 Elsevier Ltd. All rights reserved.
doi:10.1016/j.jpcs.2003.09.033

introduces the lattice anharmonicity and modulates the electron–lattice interaction, and therefore, the pairing strength in the metallic units.

The separation between the boron layers is a relevant structural parameter since it controls the band dispersion along the *c*-axis direction and therefore, it controls the T_c via both the 2D–3D cross-over of the Fermi surface and the induced variation of the density of states (DOS).

The introduction of holes or electrons into MgB_2 through the replacement of divalent Mg by a metal atom, having lower (or higher) valence, changes the charge density in the boron layers and the Fermi level is shifted downward (or upward). Moreover, the variation of the intercalated ions between the boron honeycomb monolayers modifies both the transversal dispersion (by changing the spacing) and the electron–lattice interaction (by varying the micro-strain).

Therefore, chemical substitution is an effective way to determine the effect of each of these parameters on the electronic properties of the system. Consequently, during the last two years several attempts of chemical substitution in MgB_2 were made [2]. However, a complete substitution was obtained only in the case of Al replacing Mg [10–15] and C replacing B [16]. In all the other cases the substitution for Mg and B was partial and often dubious [17].

Al is a trivalent metal with a much smaller atomic radius than Mg, thus the substitution of Mg by Al results not only in the addition of electrons but also in a compression of the MgB_2 lattice structure.

On contrary Sc and Mg have nearly the same atomic radius, therefore, the synthesis and investigation of the $Mg_{1-x}Sc_xB_2$ section are very useful and of great relevance because it can allow the study of the band filling effect on the superconducting properties with a minimum effect on the structure size. With this motivation, we have studied the $Mg_{1-x}Sc_xB_2$ section in order to explore the influence of charge density on the electronic properties. Until now MgB_2 have been considered insoluble with ScB_2 [17]. Here, we show for the first time that by optimizing the preparation conditions a solid solution $Mg_{1-x}Sc_xB_2$ can be synthesized. In this paper, we have reported characterization of several $Mg_{1-x}Sc_xB_2$ samples of their structural and superconducting properties using X-ray diffraction (XRD) and complex conductivity measurements. On the basis of the results shown we argue that the holes in the boron σ bands play an essential role for the occurrence of superconductivity in the diborides.

1. Experimental

Several samples along the $Mg_{1-x}Sc_xB_2$ section were synthesized by direct reaction of the elemental magnesium and scandium (powder, 99.9 mass% nominal purity) and boron (99.5% pure <60 mesh powder). The starting materials were mixed in the stoichiometric ratio and pressed into a pellet of 8 mm in diameter. The pellet was enclosed in tantalum crucible and sealed by arc welding under argon atmosphere. The Ta crucibles were then heated in a furnace Centorr M60 under high-pure Ar atmosphere for 5 min at 1280 °C, 2 h at 1150 °C, 6 h at 1050 °C and 6 h at 950 °C. An important improvement in the synthesis process was that of avoiding use of quartz tube (unlike Ref. [14] where quartz was used) since the Mg gas at high-temperature reacts with quartz and induces a MgO impurity phase in the final compound.

The samples were characterized for their superconducting properties by the temperature dependence of the complex conductivity using the single-coil inductance method [18]. The measurement system contains a simple electronic circuit constituted of a capacitance C, connected in parallel to a spiral coil, with an inductance L and a resistance R, that is placed on the sample surface. This circuit is mounted in a liquid ^{3}Helium cryostat (HELIOX ^{3}He). In this experimental system the sample temperature is controlled and measured by an Oxford ITC-503 temperature controller, interfaced with a computer alongside other measuring devices.

The frequency dependent complex impedance $Z = R + i\omega L$ of the coil was measured in the experiments with a temperature dependent resonant frequency $f(T) = (2\pi)^{-1} \times [1/(L(T)C) - R(T)^2/L(T)^2]^{1/2}$ of the order of 2–5 MHz. A marginal oscillator, device that has ability to excite the tank circuit at its resonant frequency and to stabilize the oscillation amplitude $V(T)$ to a level strongly dependent on the equivalent resistance $R_{eq} = L/(RC)$ of the circuit, was used for the measurements. The resonance frequency $f(T)$ and the oscillation amplitude $V(T)$ were measured using a frequency-meter (HP53131A) and a digital multimeter (HP3478A), respectively. Temperature dependent changes in $V(T)$ and $f(T)$ due to sample contribution to the $L(T)$ (i.e. $\Delta L(T)$) and $R(T)$ (i.e. $\Delta R(T)$) were measured. Large number of experimental points were collected with a temperature resolution better than 0.1 K.

The structural properties of the samples were determined by powder XRD. The diffraction patterns were measured in the Bragg–Brentano $\theta-\theta$ geometry by a vertical X'Pert Pro MPD diffractometer using a Cu K_α radiation.

2. Results and discussion

The X-ray powder diffraction patterns measured at $T = 300$ K on samples belonging to the $Mg_{1-x}Sc_xB_2$ section for different Sc concentrations are shown in Fig. 1a. All the peaks are indexed according to the hexagonal AlB_2 structure type (*P6/mmm* space group). A minority phase of metallic Mg is observed in the MgB_2 sample, while very little impurity phases of MgB_4 ($<4\%$) and MgO ($<1\%$) are present in the Sc-doped samples. The (110) line exhibits a systematic shift with scandium substitution. This trend can be better observed in Fig. 1b where the (110) peak is shown enlarged. For low Sc content

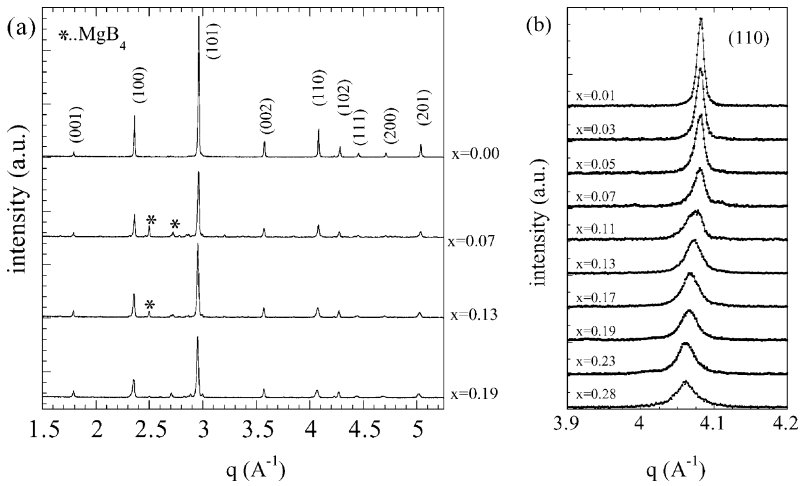

Fig. 1. (Panel a) X-ray powder diffraction patterns measured at $T = 300$ K on $Mg_{1-x}Sc_xB_2$ system for different Sc content. (Panel b) Evolution of (100) peak as function of Sc content.

the peak is asymmetric due to the coexistence of two phases with different Sc concentration: the phase 1 corresponds to the peak with higher q value and to an a-axis close to that of MgB_2 (3.085 Å); the phase 2 with the peak at lower q value and has an a-axis intermediate between that of MgB_2 and ScB_2 (3.141 Å).

From XRD data it is clear that for low Sc concentration ($0.01 \leq x < 0.13$) there is a miscibility gap where a $Mg_{1-x}Sc_xB_2$ phase coexists with a MgB_2 nearly pure phase, indicating that the miscibility of ScB_2 in MgB_2 is only partial. A minor amount of MgB_2 phase is present ($\sim 10\%$) for a Sc concentration of $x > 0.07$ and nearly disappears for $x > 0.13$.

The diffraction patterns have been analysed by standard least squares refinement (Rietveld method) in order to determine the lattice parameters and to study their dependence on Sc content. The GSAS program has been used for this fitting procedure. Special care has been taken to check the positions of the MgB_4 impurity peaks in order to have results independent of diffractometer calibration errors.

The variations of the a- and c-axes as a function of Sc content x are plotted in Fig. 2. By increasing Sc content x, a small linear elongation of a-axis is observed while the c-axis is nearly constant. The miscibility gap is indicated by a dashed region.

The temperature dependence of f_0^2/f^2, probing radio frequency conductivity, measured on $Mg_{1-x}Sc_xB_2$ system for several Sc contents is shown in Fig. 3. In the low Sc concentration range $0.01 \leq x < 0.13$ a double superconductive transition is observed due to the existence of two phases with different Sc content. With increasing the Sc content from $x = 0.13$ to 0.33 the superconductive transition shifts to lower temperatures.

The superconducting properties appear to have a clear analogy with the diffraction measurements: both measurements show the presence of a two phase region at low Sc content and we could associate the high T_c phase to the phase 1, determined by diffraction, with an a-axis close to that of MgB_2, and the lower T_c phase to the phase 2 with a higher a-axis. Therefore, it was possible to make a one to one correspondence between the lattice and the superconductive properties of the different phases.

In Fig. 4 we have plotted the superconducting transition temperature as a function of the a-axis. The T_c shows a gradual decrease with an increase in the a-axis, albeit with a sharp change at the $a \sim 3.093$ Å.

This anomalous behaviour cannot be explained by the a lattice parameter expansion. In fact a linear Sc content

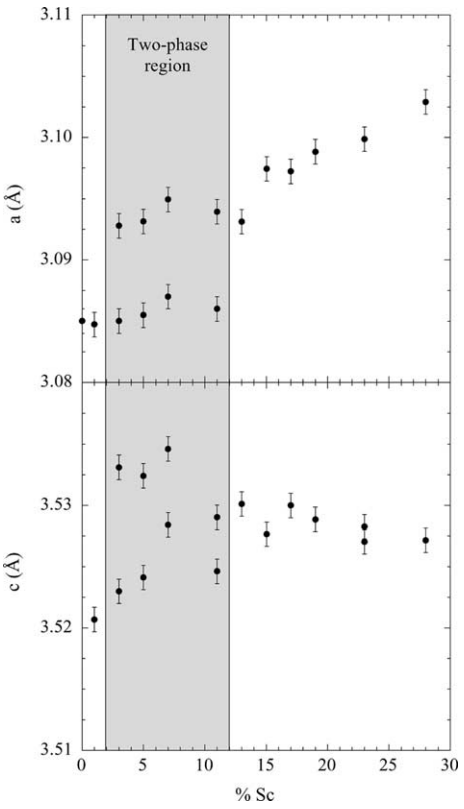

Fig. 2. Variation of a- and c-axes as a function of Sc doping x in $Mg_{1-x}Sc_xB_2$ samples.

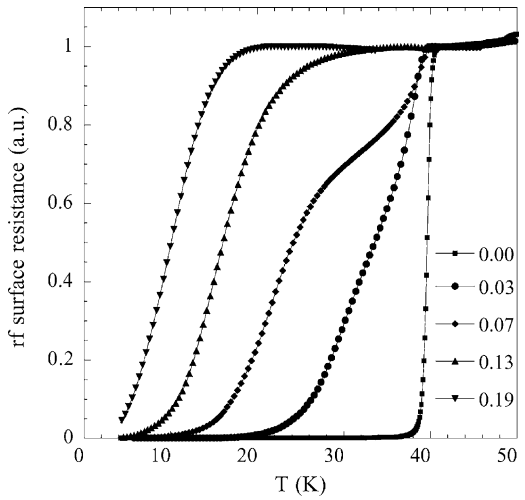

Fig. 3. Radio frequency conductivity probed by the ratio f_0^2/f^2, where, $f_0(T)$ and $f(T)$ are the resonance frequencies of the probing LC circuit measured without and with the sample, respectively. The ratio f_0^2/f^2 is measured on $Mg_{1-x}Sc_xB_2$ samples with different values of x.

dependence without structural transition or anomalies is shown in Fig. 5 by the average values of the a-axis of the different coexisting phases, each a value weighted with the corresponding phase fraction (Table 1). Therefore, in order to explore the origin of the sharp change of the T_c, it is necessary to determine the Sc content at which this superconductive transition occurs. It should be pointed out that in the two-phase region the real Sc concentrations of the high T_c and low T_c phases are greater and lesser than the stoichiometric one. By fitting with a linear function the Sc content dependence on the mean a-axis, we have estimated the real Sc concentration in each phase.

The evolution of the critical temperature for the superconductivity in the $Mg_{1-x}Sc_xB_2$ has been reported in Fig. 6a as a function of the estimated Sc content x : the T_c shows various regimes by increasing x. A high T_c regime ($39.5\ K > T_c > 30\ K$) is present for $0 < x < 0.14$, where

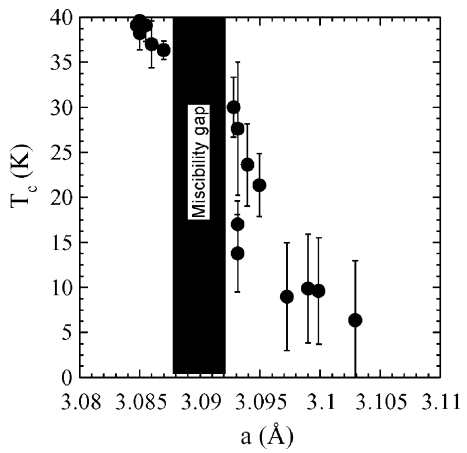

Fig. 4. Critical temperature T_c plotted as a function of the corresponding a-axis.

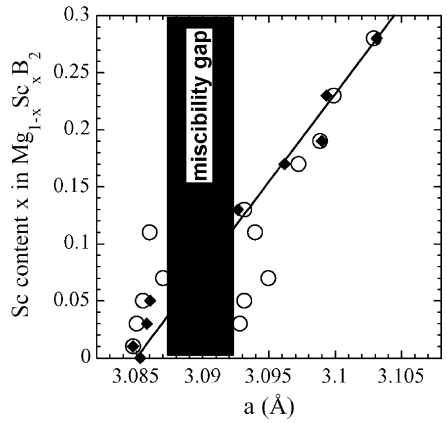

Fig. 5. Mean of the a-axis of the different coexisting phases, each a value weighted with the corresponding phase fraction.

the critical temperature shows a slow nearly linear decrease with the increase in Sc content. On contrary, at $x \sim 0.15$, the T_c exhibits a jump towards a low T_c superconductivity regime ($15 > T_c > 5$ K). The superconductivity disappears in the proximity of $x = 0.30$. The T_c behaviour can be explained by considering the electronic band structure. The small changes in the lattice size between MgB_2 and ScB_2 compounds indicates that the effect of substituting Sc for the Mg can be believed primarily as a simple filling of available electronic states, with one electron donated per Sc, within the rigid band picture.

The DOS at the Fermi level as a function of the electron addition to the MgB_2 system is illustrated in Fig. 6b. The calculations show that the DOS decreases suddenly at an electron concentration analogous to the one where the jump in the T_c is observed. Therefore, it can be concluded that the sharp drop of the T_c in the low T_c regime is associated with the decrease of the DOS at the Fermi level. The effect of the drop of the DOS on the T_c is evident in same Fig. 6b, where we have reported the T_c predicted by the BCS single band theory using the DOS calculated by An and Pickett [8].

The critical electron doping of $x = 0.25$, at which the number of holes in the σ bands vanishes, is only slightly lower than the Sc concentration where the superconductivity is suppressed. Consequently, the observed loss of the superconductivity in the $Mg_{1-x}Sc_xB_2$ system can be explained as a result of the filling of the σ bands. However, for Sc concentration higher than $x = 0.15$, the experimental T_c diverges from the T_c predicted by the BCS single band theory which we think to be due to interchannel pairing near a shape resonance [19].

In summary, we have studied the $Mg_{1-x}Sc_xB_2$ system as a function of Sc content, in order to determinate the effect of charge density on its superconducting properties. The T_c decreases by increasing the Sc doping and the superconductivity disappears near a critical doping values of 0.30. Theoretical band structure calculations show that at this

Table 1
a- and *c*-axes values of the three phases

x	$a_1 \pm 0.001$ (Å)	$a_2 \pm 0.001$ (Å)	$a_3 \pm 0.001$ (Å)	$c_1 \pm 0.001$ (Å)	$c_2 \pm 0.001$ (Å)	$c_3 \pm 0.001$ (Å)	$c \pm 0.001$ (Å)	$P_1 \pm 5\%$	$P_2 \pm 5\%$	$P_3 \pm 0.1\%$
0.00	3.085	/	/	3.521		/	–	100	0	0.0
0.01	3.085	3.090	/	3.521	3.531	/	–	95	5	0.0
0.03	3.085	3.092	/	3.523	3.533	/	–	88	10	0.0
0.05	3.086	3.093	/	3.524	3.532	/	–	91	7	0.0
0.07	3.087	3.095	/	3.528	3.535	/	–	72	22	0.0
0.11	3.086	3.094	/	3.525	3.529	/	–	30	66	0.0
0.13	3.088	3.093	/	3.527	3.530	/	–	9	87	0.0
0.17	3.088	3.097	/	–	–	3.530	–	11	86	0.0
0.19	/	3.098	/	/	3.530	/	–	0	98	0.0
0.23	3.082	3.101	3.141	–	–	3.520	3.527	12	82	4.0
0.28	3.084	3.103	3.141	–	–	3.520	3.527	15	72	8.0

In the samples where it was not possible to distinguish the *c*-axes of the phases 1 and 2 a unique value is reported in the column labeled 'c'. The corresponding phase fraction (P_1, P_2, P_3) is also reported.

critical doping value the boron σ bands are filled. Consequently, the superconductivity loss observed in the $Mg_{1-x}Sc_xB_2$ system can be explained as a result of the filling of the σ bands. However, as Sc content increases, the experimental T_c diverges from the T_c predicted by the BCS single band theory indicating a new mechanism must be considered.

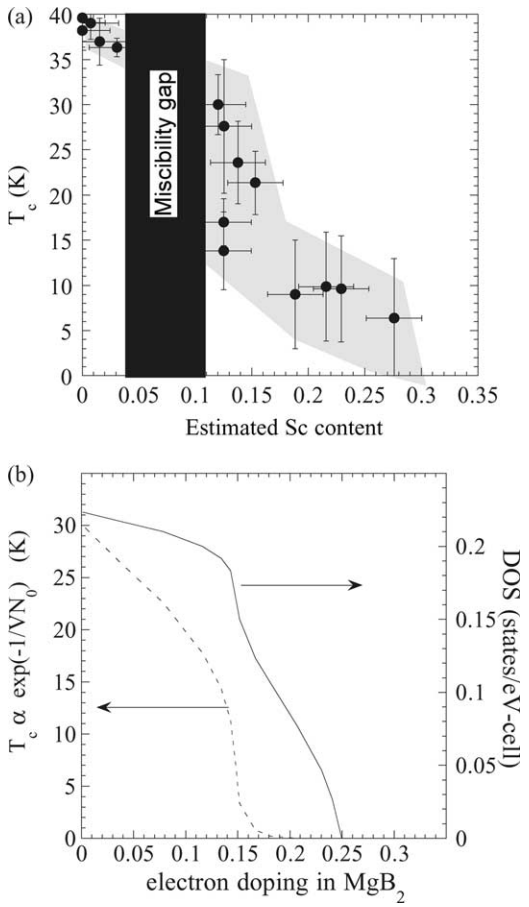

Fig. 6. (Panel a) Evolution of the critical temperature as a function of the estimated Sc content x. (Panel b) Density of states at the Fermi level (dotted line) and number of holes per unit cell n_h (solid line) in the σ bands as a function of the electrons added to MgB_2 [8].

Acknowledgements

This work was supported by MIUR in the frame of the project 'Leghe e composti intermetallici: stabilità termodinamica, proprietà fisiche e reattività', by 'Istituto Nazionale Fisica della Materia' (INFM), and by 'Consiglio Nazionale delle Ricerche' (CNR) in the frame of the project '5% superconduttività'.

References

[1] J. Nagamatsu, N. Nakagawa, T. Muranaka, Y. Zenitani, J. Akimitsu, Nature 410 (2001) 63.
[2] C. Buzea, T. Yamashita, Supercond. Sci. Technol. 14 (2001) R115.
[3] W.L. McMillan, Phys. Rev. 167 (1968) 331.
[4] B. Lorenz, R.L. Meng, Y.Y. Xue, C.W. Chu, Phys. Rev. B 64 (2001) 52513.
[5] G. Satta, G. Profeta, F. Bernardini, A. Continenza, S. Massidda, Phys. Rev. B 64 (2001) 104507.
[6] S. Suzuki, S. Higai, K. Nakao, J. Phys. Soc. Jpn 70 (2001) 1206.
[7] J.B. Neaton, A. Perali, cond-mat/0104098, 2001.
[8] J.M. An, W.E. Pickett, Phys. Rev. Lett. 86 (2001) 4366.
[9] J. Kortus, I.I. Mazin, K.D. Belashchenko, V.P. Antropov, L.L. Boyer, Phys. Rev. Lett. 86 (2001) 4656.
[10] S. Agrestini, D. Di Castro, M. Sansone, N.L. Saini, A. Saccone, S. De Negri, M. Giovannini, M. Colapietro, A. Bianconi, J. Phys.: Condens. Matter 13 (2001) 11689.
[11] A. Bianconi, D. Di Castro, S. Agrestini, G. Campi, N.L. Saini, A. Saccone, S. De Negri, M. Giovannini, J. Phys.: Condens. Matter 13 (2001) 7383.
[12] A. Bianconi, S. Agrestini, D. Di Castro, G. Campi, G. Zangari, N.L. Saini, A. Saccone, S. De Negri, M. Giovannini, G. Profeta, A. Continenza, G. Satta, S. Massidda, A. Cassetta, A. Pifferi, M. Colapietro, Phys. Rev. B 65 (2002) 174515.
[13] D. Di Castro, S. Agrestini, G. Campi, A. Cassetta, M. Colapietro, A. Congeduti, A. Continenza, S. De Negri, M. Giovannini, S. Massidda,

M. Nardone, A. Pifferi, P. Postorino, G. Profeta, A. Saccone, N.L. Saini, G. Satta, A. Bianconi, Europhys. Lett. 58 (2002) 278.
[14] J.S. Sluski, N. Rogado, K.A. Regan, M.A. Hayward, P. Khalifah, T. He, K. Inumaru, S. Loureiro, M. Haas, H.W. Zandbergen, R.J. Cava, Nature 410 (2001) 343.
[15] J.Q. Li, L. Li, F.M. Liu, C. Dong, J.Y. Xiang, Z.X. Zhao, Phys. Rev. B 66 (2002) 012511.
[16] A. Bharathi, S. Jemima Balaselvi, S. Kalavathi, G.L.N. Reddy, V.S. Sastry, Y. Hariharan, T.S. Radhakrishnan, Physica C 370 (2002) 211.
[17] R.J. Cava, H.W. Zandbergen, K. Inumaru, Physica C 385 (2003) 8.
[18] D. Di Castro, N.L. Saini, A. Bianconi, A. Lanzara, Physica C 332 (2000) 405.
[19] A. Bussmann-Holder, A. Bianconi, Phys. Rev. B 67 (2003) 132509.